

Article

# SWAT-Simulated Streamflow Responses to Climate Variability and Human Activities in the Miyun Reservoir Basin by Considering Streamflow Components

Tiezhu Yan <sup>1</sup>, Jianwen Bai <sup>1,2</sup>, Amelia LEE ZHI YI <sup>3</sup> and Zhenyao Shen <sup>1,\*</sup> 

<sup>1</sup> State Key Laboratory of Water Environment Simulation, School of Environment, Beijing Normal University, Beijing 100875, China; yanxiaoshi1984@126.com (T.Y.); baijw@jlnu.edu.cn (J.B.)

<sup>2</sup> College of Environmental Science and Engineering, Jilin Normal University, Siping 136000, China

<sup>3</sup> Soil and Water Management and Crop Nutrition Laboratory, Joint FAO/IAEA Division of Nuclear Techniques in Food and Agriculture, IAEA, Seibersdorf 2444, Austria; a.lee-zhi-yi@iaea.org

\* Correspondence: zyshen@bnu.edu.cn; Tel.: +86-10-5880-0398

Received: 9 December 2017; Accepted: 8 March 2018; Published: 23 March 2018



**Abstract:** The streamflow into Miyun Reservoir, the only surface drinking water source for Beijing City, has declined dramatically over the past five decades. Thus, the impacts of climate variability and human activities (direct and indirect human activities) on streamflow and its components (baseflow and quickflow) needs to be quantitatively estimated for the sustainability of regional water resources management. Based on a heuristic segmentation algorithm, the chosen study period (1969–2012) was segmented into three subseries: a baseline period (1969–1979) and two impact periods I (1980–1998) and II (1999–2012). The Soil and Water Assessment Tool (SWAT) was adopted to investigate the attributions for streamflow change. Our results indicated that the baseflow accounted for almost 63.5% of the annual streamflow based on baseflow separation. The contributions of climate variability and human activities to streamflow decrease varied with different stages. During impact period I, human activities was accountable for 54.3% of the streamflow decrease. In impact period II, climate variability was responsible for 64.9%, and about 8.3 mm of baseflow was extracted from the stream on average based on the comparison of the observed streamflow and simulated baseflow. The results in this study could provide necessary information for water resources management in the watershed.

**Keywords:** climate variability; human activities; baseflow separation; Miyun Reservoir basin; hydrological modeling; streamflow components

## 1. Introduction

It has been shown that the effects arising from global warming modify the precipitation pattern, which further affects the hydrological processes, with possible unfavorable effects on regional ecological environments that are dependent on these resources [1,2]. In addition, the hydrologic processes are also modulated by human activities, mainly including the construction and operation of hydraulic engineering (e.g., reservoirs), water withdrawal for population growth, agricultural development and industrial development and land use/cover change [3–5]. Thus, climate variability and human activities are two major driving factors influencing the hydrological processes and spatio-temporal distribution of water availability. Streamflow, which is a combination of hydrological cycles in the routing phase and in the land phase, has often been adopted as an indicator of hydrological responses to climate variability and human activities at the watershed scale [6,7]. From the perspective of regional water resources sustainability, it is imperative to ascertain the impacts of climate variability

and human activities on streamflow change and determine their relative contributions at the watershed level. Therefore, the quantitative identification of the influences of climate variability and human activities on streamflow change at the basin level has already become an active research area [8,9].

Due to the fact that streamflow responses to climate variability and human activities vary in different basins, some studies have been done to assess the streamflow responses to these two kinds of factors at the watershed scale [9–12]. Previous researches focused on the response of the total streamflow to climate variability and human activities in a watershed. As we know, streamflow can be divided into baseflow and quickflow (or direct runoff) [13,14]. Quickflow is the high frequency flow which is the sum of surface runoff and lateral flow [15]. The role of each streamflow component, especially baseflow, is of importance for the river ecosystem stability and health [16]. Therefore, streamflow components need to be incorporated into the study of the response of streamflow to climate variability and human activities for regional water resources management [17].

Many techniques have been utilized for identifying the impact of climate variability and human activities on streamflow change at the watershed scale. These methods can be classified as experimental approaches, hydrological modeling, conceptual approaches and analytical approaches [8,18]. Considering simulations of streamflow components, the method of physically-based hydrological modeling was chosen to establish a link between hydrological processes and external forcings at the watershed scale. Among the existing hydrologic models, the performance of baseflow simulation of the Soil and Water Assessment Tool (SWAT) model has been validated around the world [17,19–21]. Therefore, the SWAT model was adopted. Meanwhile, a realistic description of different streamflow components is crucial for capturing the hydrological processes in a watershed and reducing the uncertainties arising from the modeling [21,22].

The Miyun Reservoir is the only surface source of drinking water for Beijing City [23,24] (Figure 1). The annual runoff from its upstream basin, namely the Miyun Reservoir Basin (MRB), into the reservoir has declined significantly over the last five decades, especially after the year 2000. Furthermore, the streamflow decreases have seriously affected Beijing's water supply [25,26] and threatened the sustainability of the regional ecological environment [24,27]. Identifying the major cause for the streamflow reduction in the MRB has been done recently [23,25,28,29]. The studies conducted by Ma et al. [25] and Zhao et al. [28] illustrated that the climate variability was accountable for about 51–55% and 63.24% of decrease in reservoir inflow, respectively while Wang et al. [23] concluded that the decrease in runoff can be attributed to about 35% from climate variability in the MRB. In addition, the direct human activities (i.e., the changes in land use and land cover) are also considered in the hydrological responses to climate variability and human activities [25,28,29]. However, these studies have not converged to a consensus regarding their conclusions. Meanwhile, these studies mainly focused on total streamflow into the Miyun Reservoir. The impacts of climate variability and human activities (direct and indirect human activities) on the streamflow's components, baseflow and quickflow, have not yet been reported. It is a matter of great urgency for policymakers to fully understand the impacts of climate variability and human activities on the changes in streamflow and its components from the viewpoint of sustainable water resources management.

The primary goals of this paper are: (1) to identify the abrupt change (herein referred to as breakpoint) of annual streamflow and analyze the variations in hydroclimatic variables in the watershed; (2) to determine the individual impact of climate variability and human activities on streamflow change as well as their relative contributions in the MRB; (3) to further analyze the impact of human activities (indirect and direct human activities) on the streamflow by considering streamflow components based on the baseflow separation.

## 2. Study Area and Dataset

### 2.1. Study Area Description

The MRB, with a drainage area of about 15,350 km<sup>2</sup>, extends from 40°19'N to 41°38'N latitude and from 115°25'E and 115°35' E longitude. The watershed is in the upstream of the Haihe River Basin (HRB) in northern China. The watershed mainly includes four counties of Fengning, Chicheng, Luanping and Xinglong in Hebei province and three counties of Miyun, Huairou and Yanqing in Beijing City. The Chao and Bai Rivers, two tributaries in the watershed, cover 6220 km<sup>2</sup> and 9130 km<sup>2</sup>, respectively (Figure 1). Both originate from the mountainous area in the Hebei province; they run southeast until they enter into the Miyun Reservoir. The watershed is characterized by a continental monsoon climate with the mean annual temperature of 7.5 °C and the annual precipitation of 487 mm, respectively [26]. The intra-annual distribution of precipitation is uneven; more than 80% of the annual precipitation falls during the flood season (June to September). The average annual streamflow is about  $6.3 \times 10^8$  m<sup>3</sup> during the period of 1969–2012. The intra-annual distribution of streamflow is similar to that of precipitation due to the precipitation-driven hydrological processes in the MRB (Figure 2).

Human activities in the MRB mainly include land use change, the construction and operation of the hydraulic engineering, water withdrawal for population growth, agricultural development and industrial development. Massive afforestation programs, including the Three-North Shelter Forest Program, the Greening Project of the Taihang Mountains, and the Beijing and Tianjin Sand Source Control Project were introduced in the MRB. Consequently, forested areas increased from 49.2% in the 1980s to 65.7% in 2000, whereas agriculture and pasture areas decreased from 21.2% and 27.3% to 16.3% and 15.7%, respectively (Supplementary Figure S1). Meanwhile, there are four main reservoirs in the MRB with the total storage capacity of about 2.21 billion m<sup>3</sup>: Yunzhou, Baihepu, Banchengzi and Yaoqiaoyu reservoirs with the total storage capacity of  $1.02 \times 10^9$  m<sup>3</sup>,  $0.90 \times 10^9$  m<sup>3</sup>,  $0.10 \times 10^9$  m<sup>3</sup>, and  $0.19 \times 10^9$  m<sup>3</sup>, respectively (Figure 1). Detailed information related to these reservoirs is described in the Supplementary Table S1. After 1999, the MRB experienced constant aridity, which arose from a shortage of precipitation. The joint operation of the reservoir group was performed with the aim of ensuring downstream water security since 2003.

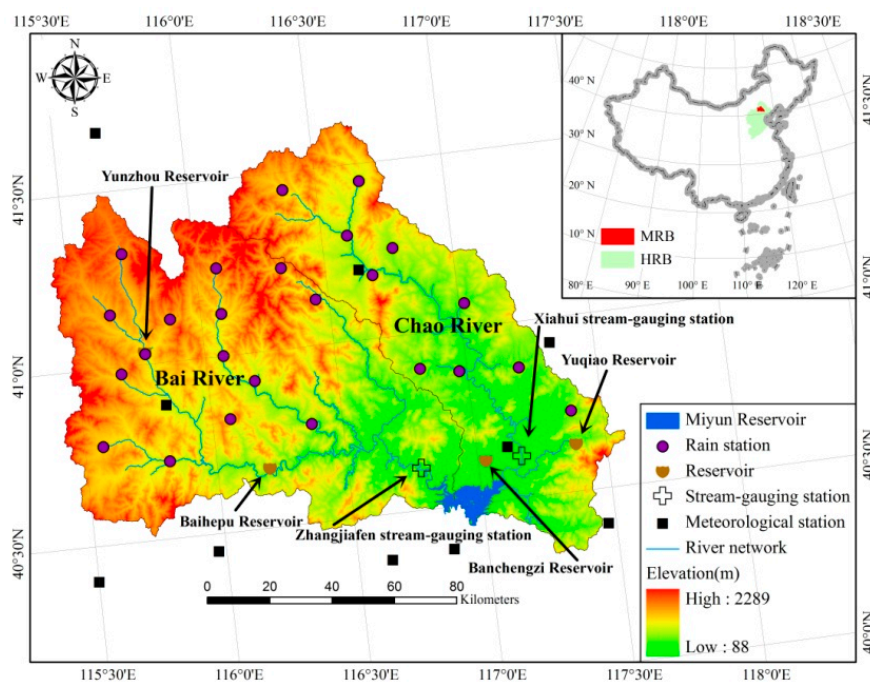
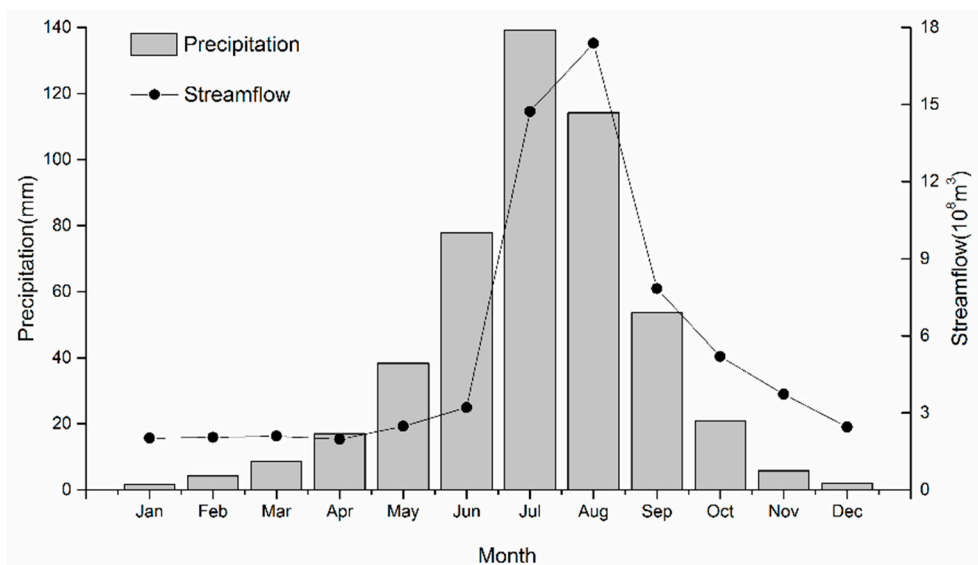


Figure 1. Location of the MRB and hydroclimatic stations.



**Figure 2.** Intra-annual distribution of precipitation and streamflow based on observations from 1969 to 2012.

## 2.2. Datasets Used in This Study

In this study, datasets were used for the baseflow separation and SWAT setup. The major input geospatial data used for the SWAT simulation included: (1) a 1:1,000,000 China Soil Map; (2) land-use maps (1: 25,000) for the 1980s and 2000; (3) a 90 m Digital Elevation Model (DEM); (4) daily climate data of 1969–2012 from 11 meteorological stations and 25 rain gauges (Supplementary Table S2). These geospatial datasets of different resolutions were converted to a common resolution raster of 90 m using the Resample Tool in ArcGIS 9.3 software package [30,31]. Monthly observed runoff data for years 1969–2012 at the Zhangjiafen stream-gauging station in the Bai River and Xiahui stream-gauging station in the Chao River, respectively, were also collected. The sources of these input data are listed in Table 1. In addition, daily runoff data from 1969 to 1979 at the above two stream-gauging stations were collected for the baseflow separation. Recognizing the annual patterns of precipitation and streamflow in the MRB (Figure 2), we divided the year into flood season and non-flood season. The flood season was from June to September; the non-flood season included the other months [32].

**Table 1.** Input data for the Soil and Water Assessment Tool (SWAT) model.

Data Type	Data Sources
DEM	The National Geomatics Center of China
Soil map	China Soil Map based Harmonized World Soil Database from Environmental and Ecological Science Data Center for West China
Land cover	Institute of Geographical Sciences and Natural Resources Research, Chinese Academy of Science
Climate data	Daily climatic data from 11 stations from the National Climatic Centre of China Meteorological Administration; Daily precipitation data from 25 rain gauges from the Hydrologic yearbook
Discharge data	Observed data from the Xiahui and Zhangjiafen stream-gauging stations from the Hydrologic Yearbook

## 3. Methodologies

### 3.1. Framework for Identifying the Impacts of Climate Variability and Human Activities on Streamflow Change

Generally, the factors which cause the runoff variation in a watershed can be delineated into two parts: human activities and climate variability. These two parts are regarded as independent, although climate variability and human activities interact with each other in the real world. Thus, the total

runoff change ( $\Delta Q$ ) under the common influences of climate variability and human activities, can be estimated by the following equation [33,34]:

$$\Delta Q = \Delta Q_C + \Delta Q_H \quad (1)$$

where  $\Delta Q_C$  and  $\Delta Q_H$  represent runoff change induced by climate variability and human activities, respectively.

Firstly, the historical runoff time series needs to be separated into two segments. The first one denotes the baseline period impacted only by climate variability, while the second one represents the runoff change period (herein referred to as impact period) under the combined impacts of climate variability and human activities (Figure 3).  $\Delta Q$  represents the difference in the measured runoff between impact period and baseline period, according to the following equation.

$$\Delta Q = \bar{Q}_{obs}^2 - \bar{Q}_{obs}^1 \quad (2)$$

where  $\bar{Q}_{obs}^1$  and  $\bar{Q}_{obs}^2$  are the observed average runoff during baseline period and impact period, respectively.

Secondly, the method for the reconstruction of the nature runoff during impact period was adopted to determine  $\Delta Q_H$  according to the following equation:

$$\Delta Q_H = \bar{Q}_{obs}^2 - \bar{Q}_{sim}^2 \quad (3)$$

where  $\bar{Q}_{obs}^2$  and  $\bar{Q}_{sim}^2$  are the observed and reconstructed mean runoff during impact period, respectively.

Finally, the change in runoff induced by climate variability ( $\Delta Q_C$ ) was calculated based on Equation (1).

According to whether or not human activities exert an impact on the hydrological processes in the land phase, human activities can be classified into two categories: direct and indirect [25,35]. Indirect human activities mainly include any of the land use/cover changes, such as the afforestation projects, and soil and water conservation projects, which mainly influence the hydrological processes in the land phase, further influencing streamflow. Direct human activities refer to all human activities expect land use/cover changes, such as dam construction and reservoir operation, surface and groundwater withdrawal for population growth, agricultural development and industrial development.

As for human activities, the streamflow change attributed to human activities is the sum of streamflow change caused by direct human activities ( $\Delta Q_{direct}$ ) and indirect human activities ( $\Delta Q_{indirect}$ ), respectively, in the following equation.

$$\Delta Q_H = \Delta Q_{direct} + \Delta Q_{indirect} \quad (4)$$

$$\Delta Q_{indirect} = \bar{Q}_{sim1}^2 - \bar{Q}_{sim2}^2 \quad (5)$$

where  $\Delta Q_{indirect}$  and  $\Delta Q_{direct}$  represent runoff change induced by indirect and direct human activities, respectively.  $\bar{Q}_{sim1}^2$  is the simulated mean runoff using climate data during impact period.  $\bar{Q}_{sim2}^2$  is the simulated mean runoff using both land use and climate data during impact period. Finally, the runoff change induced by direct human activities ( $\Delta Q_{direct}$ ) was calculated by the difference between  $\Delta Q_H$  and  $\Delta Q_{indirect}$  based on the Equation (4).

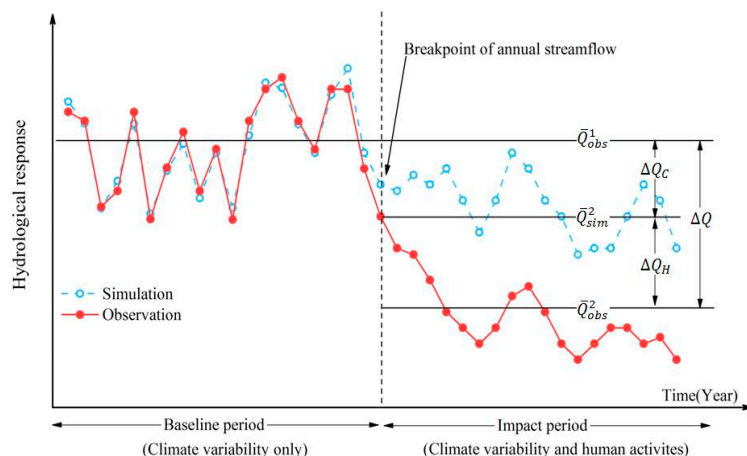


**Figure 3.** A diagrammatic plot for identifying the impacts of climate variability and human activities on streamflow change at the watershed level.

### 3.2. Detection of Hydroclimatic Changes

The analysis of the changes in hydroclimatic variables is an indispensable step for understanding the impact of climate variability on regional ecologic systems. The previous work has analyzed the trend test and trend magnitude of hydroclimatic variables, including precipitation, temperature and streamflow in the MRB [26]. Furthermore, breakpoint analysis of the annual streamflow data offered a reference to investigate the climate variability and human activities impacts on streamflow change. Traditional statistical test methods (e.g., Mann-Kendall test, sliding  $F$ -test and sliding  $t$ -test, etc.) are difficult to accurately detect the real breakpoints in the nonlinear and nonstationary time series [36–38]. However, the heuristic segmentation method developed by Bernaola-Galvan et al. [39] could deal with this problem, which is based on the thought of modified sliding  $t$ -test to detect the breakpoints of nonlinear and nonstationary time series [36]. Meanwhile, this method has been widely applied to the breakpoint detection of runoff series, such as in Wei River Basin [40], Hanjiang River Basin [41] and Yellow River Basin [42] in China. In view of the application of advantage of the heuristic segmentation method, it was adopted in this study to identify possible breakpoints of the annual runoff series in the MRB.

### 3.3. The Hydrological Model: The Soil and Water Assessment Tool (SWAT)

#### 3.3.1. SWAT Setup, Calibration and Validation

SWAT model is a watershed-scale hydrological model based on physical processes. It was developed to investigate the long-term impacts of land management practices, climate variability and land-use changes on hydrological processes, and the transportation and transformation of pollutants including the sediment and agricultural non-point pollutants at the watershed scale [43]. For SWAT setup, according to the topography and user-defined threshold drainage area, the model delineates a watershed into many sub-basins, which are further partitioned into hydrological response units (HRUs) by the overlay of soil, land use and slope characteristics in each sub-basin. Major model components include weather, hydrology, land cover/plant growth, nutrients, pesticides and land management. The HRUs are the smallest landscape unit of SWAT for hydrology processes simulation. At present the model has been applied successfully worldwide in the field of regional water resources management, pollution control and climate variability impact studies [18,44–46]. Detailed information about SWAT theory is described in Neitsch et al. [43].

In SWAT modeling, the Bai River Basin was partitioned into 45 sub-basins comprised of 664 HRUs, and the Chao River Basin has 28 sub-basins and 543 HRUs. Meanwhile, Soil Conservation Service (SCS) curve number method was used to calculate the surface runoff from daily precipitation.

The Penmann–Monteith method was used to estimate the potential evapotranspiration. For routing stream flows, the variable storage coefficient method was adopted in this study. Meanwhile, due to the shortage of data related to the operation of Yunzhou Reservoir and average annual streamflow of Yunzhou Reservoir Basin accounting for less than 6% of the corresponding value of the Bai River into Miyun Reservoir [47,48], the Yunzhou Reservoir was not considered in this study as the previous studies did [23,25,29].

The SWAT Calibration and Uncertainty Programs (SWAT-CUP), developed by Abbaspour et al. [49], was adopted for sensitivity analysis, uncertainty analysis and calibration and validation of SWAT model. Sequential Uncertainty Fitting (SUFI-2) algorithm was adopted for parameter optimization. In SUFI-2, all sources of uncertainty (including input uncertainty, structural uncertainty, parameter uncertainty) are described by parameter uncertainty with two statistics: P-factor (the percentage of observed data bracketed by 95% prediction uncertainty (95PPU), which is calculated at the 2.5% and 97.5% levels of the cumulative distribution of an output variable using Latin Hypercube Sampling) and R-factor (the thickness of the 95PPU envelop). The P-factor of 1 and R-factor of zero is a simulation that exactly corresponds to measured data. Meanwhile, SUFI-2 requires less simulations to be run to obtain the optimal parameters [50]. Based on the investigation of literature related to SWAT calibration as well as testing of sensitive parameters, the parameters to be calibrated and the initial ranges are listed in the Supplementary Table S3.

The monthly observed data (1969–1979) were segmented into two sub-series: the calibration period (1969–1974) and the validation period (1975–1979). After the calibration and validation of the SWAT during the period of 1969–1979, the calibrated parameters were considered to represent the natural hydrological processes of the MRB.

The performance of SWAT model was evaluated by the visual inspection and by statistical indicator. The coefficient of determination ( $R^2$ ), Nash-Sutcliffe efficiency ( $NSE$ ) and percent bias ( $PBIAS$ ) were adopted in this study and were calculated by the following equations:

$$R^2 = \left( \sum_1^n (O_i - \bar{O})(P_i - \bar{P}) \right)^2 / \left( \sum_1^n (O_i - \bar{O})^2 \sum_1^n (P_i - \bar{P})^2 \right) \quad (6)$$

$$NSE = 1 - \sum_1^n (P_i - O_i)^2 / \sum_1^n (O_i - \bar{O})^2 \quad (7)$$

$$PBIAS = \left( \sum_i^n (P_i - O_i) / \sum_i^n O_i \right) \times 100 \quad (8)$$

where  $P_i$  and  $O_i$  are the simulated and measured values at each time step  $i$ ;  $\bar{P}$  and  $\bar{O}$  are the mean of simulated and measured values;  $n$  denotes the total number of paired values. The range of  $NSE$  is from  $-\infty$  to 1, and  $R^2$  from 0 to 1. The model performs well when  $R^2$  and  $NSE$  values approach to 1. According to Moriasi et al. [51], the performance of SWAT model at the monthly scale can be considered as satisfactory if  $NSE > 0.5$  and  $PBIAS < \pm 25\%$ ;  $R^2$  greater than 0.6 is typically considered acceptable.

### 3.3.2. Baseflow Separation Using Automatic Baseflow Filter

In the absence of baseflow observation data, the baseflow separation methods (including graphical separation, digital filters and recession analysis) were commonly used techniques for separating baseflow from streamflow in the field of hydrology [52,53]. Among these methods, digital filter techniques could provide a subjective and repeatable estimate of baseflow, although they do not have any physical basis [54]. The digital filter method was originally used in signal analysis and

processing [55]. It assumes baseflow and quickflow as low-frequency and high-frequency signals, respectively [54]. The digital filter equations given by Lyne-Hollick [55] are described as follows:

$$q_t = \beta q_{t-1} + \frac{1 + \beta}{2} \times (Q_t - Q_{t-1}) \quad (9)$$

where  $q_t$  is the separated quickflow (or direct runoff) at the time step  $t$ ,  $Q$  is the original streamflow, and  $\beta$  is the filter parameter. Baseflow,  $b_t$ , is calculated with the following equation:

$$b_t = Q_t - q_t \quad (10)$$

where  $Q_t$  and  $q_t$  are defined as before.

In this study, the automated baseflow filter (BFLOW filter) based on Lyne-Hollick filter was developed by Arnold et al. [54]. Meanwhile, Arnold and Allen [56] concluded that automated baseflow filter technique was found to compare well with measured field estimates from six well-instrumented watersheds in USA. At present, the automated baseflow filter has been widely used in baseflow separation studies all over the world [57–60]. For example, Zhang et al. [17] used separated baseflow based on the automated baseflow filter to calibrate and validation SWAT model in the Little River Experimental Watershed, USA. Gan et al. [59] adopted the automated baseflow filter to investigate baseflow characteristics in Apline Rivers, China. Thus, the automated baseflow filter was adopted for separating baseflow from the daily streamflow data at the Xiahui and Zhangjiafen stream-gauging stations during the baseline period (1969–1979). In addition, one of output variables from this tool is Alpha Factor, which refers to baseflow recession constant and can be set as the value of ALPHA\_BF parameter to calibrate a SWAT simulation. The automated baseflow filter tool and its operation manual are available at <http://swatmodel.tamu.edu/software/baseflowfilter-program>.

In hydrological modeling, the parameters related to quickflow and baseflow calibration are interdependent with each other. Meanwhile, manual calibration for the simultaneous simulation of streamflow and its components is very time consuming [17]. Therefore, the dynamic flow separation function in the SWAT-CUP software was adopted in this study. The details of the dynamic flow separation function in the SWAT-CUP software is available in the supplementary material.

## 4. Results

### 4.1. Breakpoint Determination

The annual runoff into the Miyun Reservoir during 1969–2012 was used to identify breakpoints using the heuristic segmentation algorithm in this study. As shown in Figure 4, we can see that the annual runoff into the Miyun Reservoir fluctuated and generally decreased during the period of 1969–2012. Two significant breakpoints of the annual streamflow series happened in 1979 and 1998, respectively. These two breakpoints divide the entire study period (1969–2012) into three phases: 1969–1979, 1980–1998 and 1999–2012. The mean annual runoff depths in these three phases are 79.4 mm, 43.3 mm and 19.6 mm, respectively.

According to the breakpoint analysis along with human activities in the MRB described in the Section 2.1, the impact of human activities on streamflow change were considered to be relatively weak during the period of 1969–1979. In other word, the observed streamflow was deemed to be very close to its natural state. Thus, the period of 1969–1979 was identified as the baseline period, and the period of 1980–2012 was deemed as total impact period, which was further divided into impact periods I (1980–1998) and II (1999–2012). This showed that there were two step changes in annual streamflow during the period of 1969–2012 in the MRB.

#### 4.2. Changes in Hydroclimatic Variables

During 1969–2012, the variations in hydroclimatic variables, including annual observed streamflow, precipitation and mean temperature, are presented in Figures 4 and 5, respectively. The average annual streamflow, precipitation and mean temperature are 44.7 mm, 480 mm and 7.3 °C, respectively. The trend detection and slope estimator of hydrological variables at the seasonal and annual scales have been analyzed in our pervious study, which indicated that regional climate had gotten warmer and drier over the past 44 years [26].

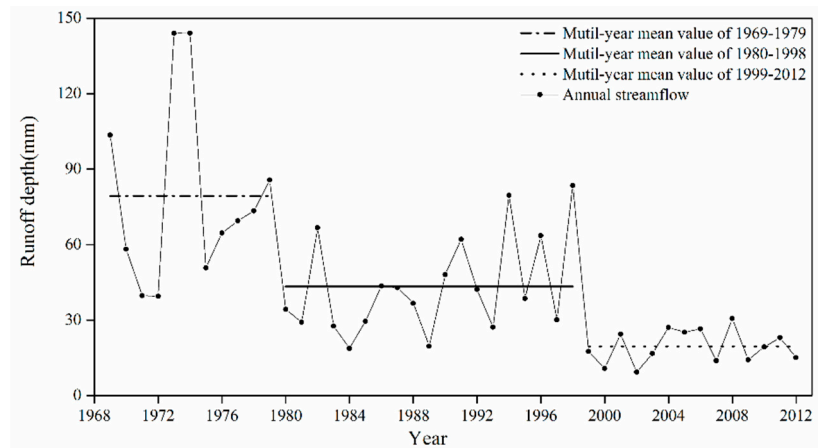


**Figure 4.** Variation in the annual runoff and its breakpoints in the MRB.

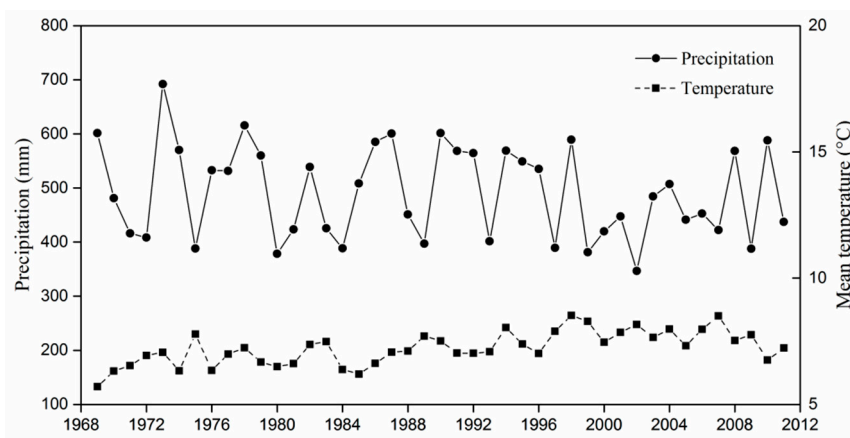


**Figure 5.** Variations in annual precipitation and mean temperature.

The average annual runoff depth, precipitation and mean temperature during the baseline period were 79.4 mm, 519.7 mm and 6.8 °C (Table 2). The changes in the runoff depth, precipitation and mean temperature during total impact period (1980–2012) were  $-46.1$  mm, and  $-46.6$  mm and  $0.6$  °C, respectively, relative to the baseline period. The annual streamflow change in the MRB shows stage changes (Figure 4). Thus, the analysis of the variability in hydroclimatic variables during different stages is critical for identifying the major driving factor for streamflow change. The changes in the runoff depth, precipitation and mean temperature during impact period I (impact period II) were  $-36$  mm ( $-59.7$  mm), and  $-29.6$  mm ( $-69.7$  mm) and  $0.4$  °C ( $1.0$  °C), respectively. It is noted that the largest decline in flood season precipitation occurred during impact period II, which was almost three times larger than the corresponding value in impact period I.

**Table 2.** Variations in the average runoff (Q), precipitation (P) and temperature (T) during different impact periods compared to the baseline period (1969–1979).

Period	Baseline Period (1969–1979)			Impact Period I (1980–1998)			Impact Period II (1999–2012)			Total Impact Period (1980–2012)		
	Q (mm)	P (mm)	T (°C)	Q (mm)	P (mm)	T (°C)	Q (mm)	P (mm)	T (°C)	Q (mm)	P (mm)	T (°C)
Annual	79.4	519.7	6.8	−36	−29.6	0.4	−59.7	−69.7	1	−46.1	−46.6	0.6
Flood season	53.9	423	19.2	−24.8	−28.5	0.4	−45.0	−90.7	1.1	−33.4	−54.9	0.7
Non-flood season	25.4	96.7	0.6	−11.2	−1.2	0.5	−14.7	21.0	0.8	−12.7	8.2	0.6

#### 4.3. Model Performance Evaluation

Based on daily streamflow data during the period of 1969–1979, streamflow was divided into baseflow and quickflow using a digital baseflow filter in this study. Figure 6 shows an example of the streamflow process and baseflow separation result at the Xiahui stream-gauging station during the baseline period in the MRB. As shown in Figure 6, the digital filter could provide extensively smooth time series of baseflow in the MRB. The result of the baseflow separation in Figure 7 shows that non-flood season streamflow arises mainly from baseflow, which accounts for more than 79.7%. While baseflow is accountable for 49 % of flood season streamflow. Overall, the baseflow contributed about 63.5% of the runoff for the whole MRB during the baseline period.

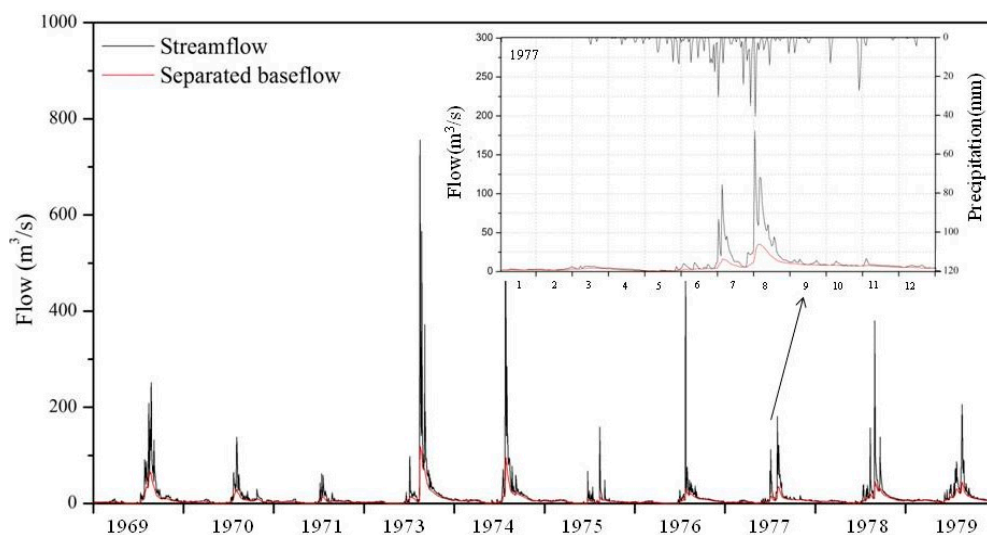


**Figure 6.** Measured streamflow and separated baseflow at the Xiahui stream-gauging station during the baseline period in the MRB.

Although the dynamic flow separation function of SWAT-CUP software could be used for simultaneous calibration of streamflow and its component, SWAT-CUP software don't output simulated values of the baseflow and quickflow for each iteration. The uncertainty analysis for baseflow and quickflow simulations could not be carried out. Therefore, we adopted P-factor and R-factor to conduct the uncertainty analysis for the streamflow here. The P-factor was 0.71 and R-factor was 0.35 in calibration period while the P-factor 0.73 and R-factor 0.59 in the validation period at Xiahui stream-gauging station. Similarly, the P-factor was 0.71 and R-factor was 0.49 in calibration period while the P-factor 0.71 and R-factor 0.74 in the validation period at Zhangjiafen stream-gauging station. The percentage of data being bracketed by 95PPU was large than 0.7 high both in calibration and validation. Additionally, some observed data were not bracketed by the 95PPU band and occurred at some peaks of streamflow, such as July in 1997 at Xiahui and Zhangjiafen stream-gauging stations.

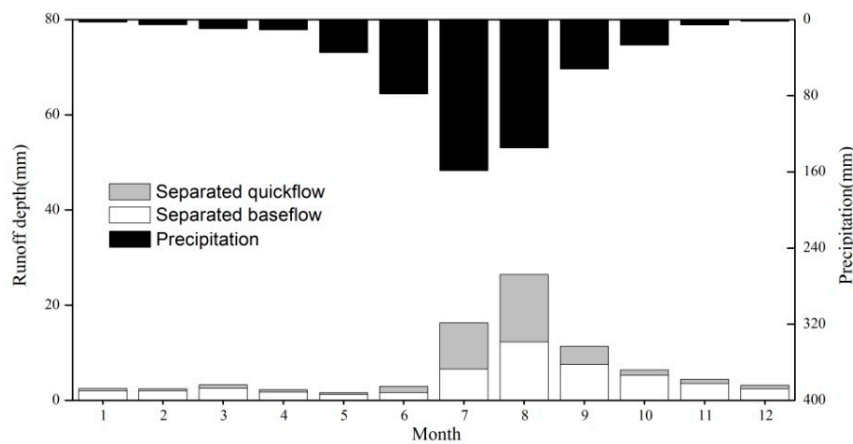


**Figure 7.** Monthly mean values of separated baseflow and quickflow for the MRB during the baseline period.

From a visual inspection by comparing the monthly separated baseflow, quickflow and observed streamflow with the corresponding simulated values for the Bai River and Chao River (Figures 8–10), the model can perform well in the timing and magnitude of most peaks in the streamflow and its components during the baseline period. In addition, three performance indicators ( $NSE$ ,  $R^2$  and  $PBIAS$ ) are presented in Table 3. The  $NSE$  and  $R^2$  values are higher than 0.63 and 0.71, and  $PBIAS$  lower than  $\pm 20\%$  for both calibration and validation periods at these two stream-gauging stations. Based on the above visual and statistical measure comparisons, the calibrated SWAT model can effectively represent hydrological processes in the MRB. In addition, Figure 11 shows that the monthly mean value of baseflow was simulated well in the MRB.

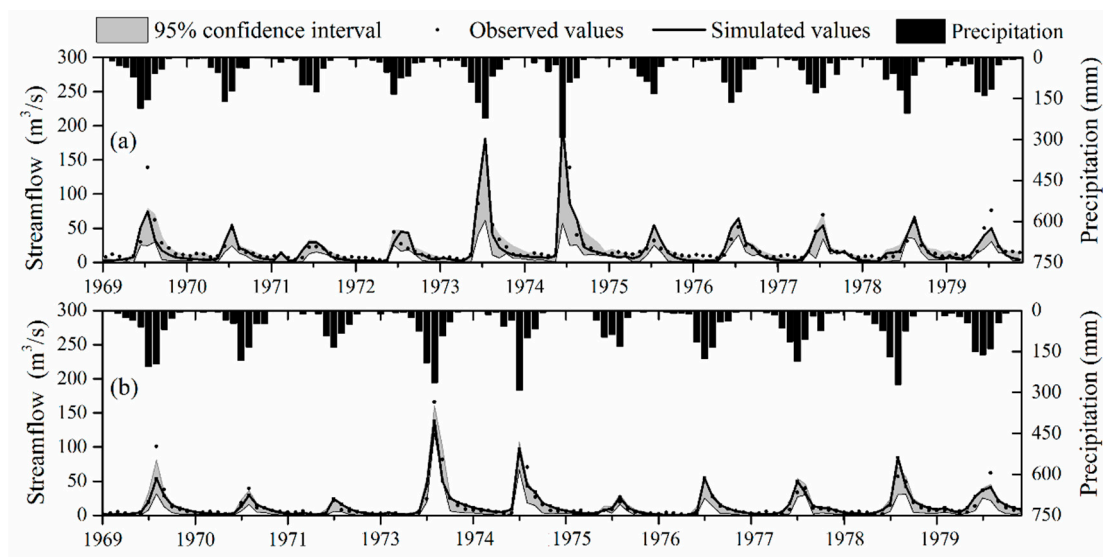


**Figure 8.** Monthly time series comparison of separated versus simulated streamflow at the Zhangjiafen (a) and Xiahui (b) stream-gauging stations in the MRB.

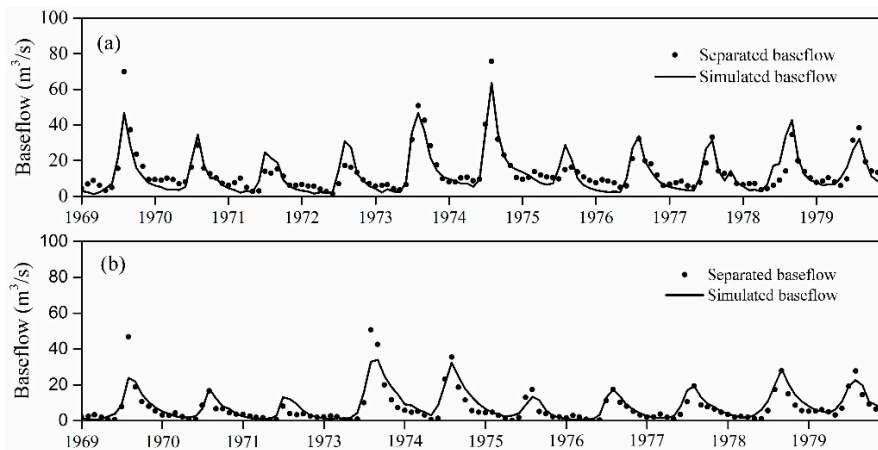


**Figure 9.** Monthly time series comparison of separated versus simulated baseflow at the Zhangjiafen (a) and Xiahui (b) stream-gauging stations in the MRB.

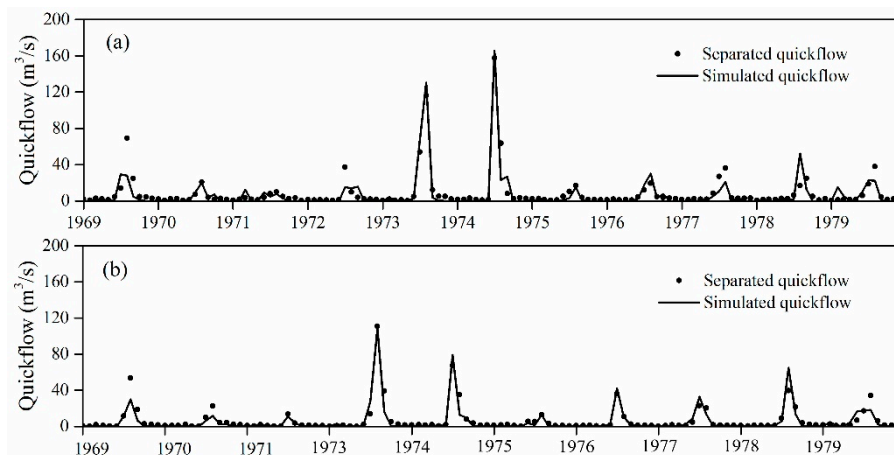


**Figure 10.** Monthly time series comparison of separated versus simulated quickflow at the Zhangjiafen (a) and Xiahui (b) stream-gauging stations in the MRB.

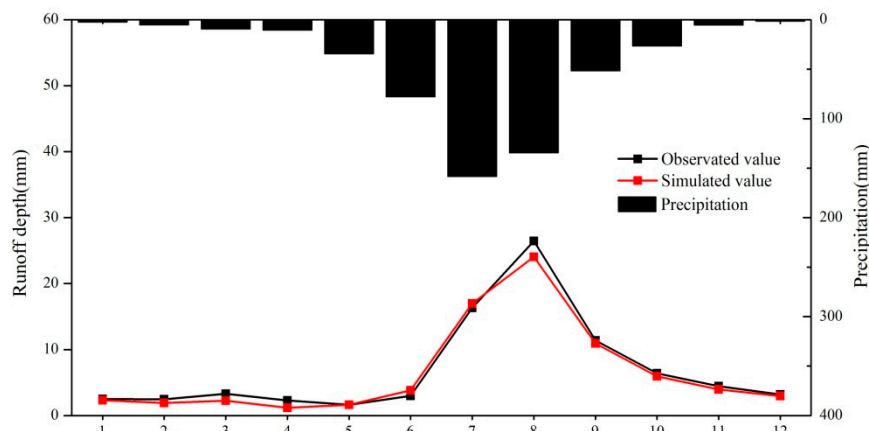


**Figure 11.** Monthly mean values of separated and simulated baseflow for the MRB during the baseline period in the MRB.

**Table 3.** Performance evaluation of the SWAT simulation.

Variables	Periods	Xiahui			Zhangjiafen		
		NSE	R <sup>2</sup>	PBIAS (%)	NSE	R <sup>2</sup>	PBIAS (%)
Baseflow (m <sup>3</sup> /s)	Calibration period	0.8	0.84	1.20	0.85	0.87	−11.00
	Validation period	0.76	0.81	19.80	0.71	0.71	−12.10
Quickflow (m <sup>3</sup> /s)	Calibration period	0.85	0.90	−19.80	0.81	0.84	−18.60
	Validation period	0.78	0.79	−9.50	0.63	0.75	−14.80
Streamflow (m <sup>3</sup> /s)	Calibration period	0.87	0.92	−10.10	0.82	0.88	−14.50
	Validation period	0.82	0.83	6.30	0.82	0.88	−13.10

Notes: Calibration period and validation period refer to the periods of 1969–1975 and 1975–1979, respectively.

#### 4.4. Assessment of the Climate Variability and Human Activities Impacts on Streamflow Change

After the model calibration and validation during the period of 1969–1979, historical climatic data obtained during total impact period (1980–2012) were utilized to reconstruct the natural runoff during different impact periods with the aim of identifying the impacts of climate variability and human activities on streamflow decrease in the MRB.

##### 4.4.1. The Impact of Climate Variability on Streamflow and Its Components

The calibrated SWAT model was performed using climate data during impact period I and II, respectively, while holding the land-use map of the 1980s unchanged. Table 4 summarizes SWAT-simulated values of streamflow and its components (baseflow and quickflow) averaged over each of different impact periods. Compared to the baseline periods, overall the streamflow and its components gradually decreased as time went on. Owing to climate variability, the average annual streamflow reduced from 74.9 mm during the baseline period to 62.9 mm and 40.6 mm in periods I and II, respectively. Similarly, the baseflow (quickflow) decreased to 40.8 mm (22.1 mm) in impact period I and 27.6 mm (13.0 mm) in impact period II from the average annual value of 47.6 mm (27.3 mm) during the baseline period. Although the streamflow and its components gradually decreased, the percentage of the baseflow in the streamflow increased from 63.5% in the baseline period to 64.8% in impact period I and 68.0% in impact period II.

**Table 4.** SWAT-simulated values of streamflow and its components averaged over each of different impact periods only considering climate variability.

Variables	Baseline Period	Impact Period I	Impact Period II
Streamflow (mm)	74.9	62.9	40.6
Baseflow (mm)	47.6	40.8	27.6
Quickflow (mm)	27.3	22.1	13.0

Notes: Baseline period, Impact period I and II refer to the sub-periods of 1969–1979, 1980–1998 and 1999–2012, respectively.

##### 4.4.2. The Impact of Human Activities on Streamflow and Its Components

Due to the shortage of land-use data, and dramatic changes in land use and land cover during impact period II [29], the impact of human activities was analyzed only for impact period II, in which the relevant results would be more effective for future regional water resources management. Thus, the calibrated model during the baseline period was implemented using the observed climate conditions during the period of 1999–2012 and the land-use map of 2000, which represent the conditions of land use/cover during impact period II.

As shown in Table 5, the SWAT-simulated average annual streamflow ( $Q_s$ ) and baseflow ( $BF_s$ ), and observed average annual streamflow ( $Q$ ) during impact period II were 36.5 mm, 27.9 mm and 19.6 mm,

respectively. During impact period II, the difference between simulated streamflow and its components using land-use maps for the 1980s (Table 4) and simulated values using land-use map of 2000 (Table 5) was caused by indirect human activities. Thus, indirect human activities caused changes of  $-4.1$  mm,  $0.3$  mm and  $-4.4$  mm of the average annual streamflow, baseflow and quickflow, respectively. The annual baseflow accounted for about 76.4% of the annual streamflow during impact period II. Due to human activities, the observed annual streamflow was less than the simulated streamflow and baseflow in each year of the period of 1999–2012. The streamflow decrease caused by direct human activities was 16.9 mm per year, which is equal to the difference between the observed average annual streamflow (19.6 mm per year) and corresponding modeled values (36.5 mm per year). In addition, the difference between observed average streamflow (19.6 mm per year) and modeled average baseflow (27.9 mm per year), using the land-use map for 2000, was 8.3 mm per year during impact period II. That is to say, baseflow decrease caused by direct human activities was 8.3 mm per year on average.

**Table 5.** SWAT-simulated values of annual streamflow and baseflow and observed annual streamflow during impact period II.

Variables	1999	2000	2001	2002	2003	2004	2005	2006	2007	2008	2009	2010	2011	2012	Mean
Q (mm)	17.5	10.8	24.5	9.3	16.7	27.1	25.2	26.5	13.9	30.6	14.3	19.4	23.0	15.1	19.6
BF <sub>s</sub> (mm)	27.0	27.4	30.0	17.3	21.9	31.0	26.9	31.1	25.8	36.8	22.2	36.9	29.1	27.0	27.9
Q <sub>s</sub> (mm)	34.7	42.8	40.7	18.6	24.9	39.4	33.0	39.5	29.2	54.3	25.5	56.6	37.9	34.0	36.5

Notes: Q, BF<sub>s</sub> and Q<sub>s</sub> stand for observed annual streamflow, simulated annual baseflow and streamflow, respectively.

As shown in Figure 12, except for February, March and November, the observed streamflow during the other months was less than the corresponding simulated baseflow. The decline in streamflow caused by human activities mainly occurred from May to October, during which the mean decrease of the percentage was more than 40%. The largest decrease in baseflow occurred in August, with a magnitude of 2.2 mm. Additionally, the observed streamflow in February, March and November were higher than the simulated streamflow because the joint operation of reservoir group, including the Baihepu, Yunzhou and Banchengzi Reservoirs, was performed with the aim of ensuring downstream water security since 2003.

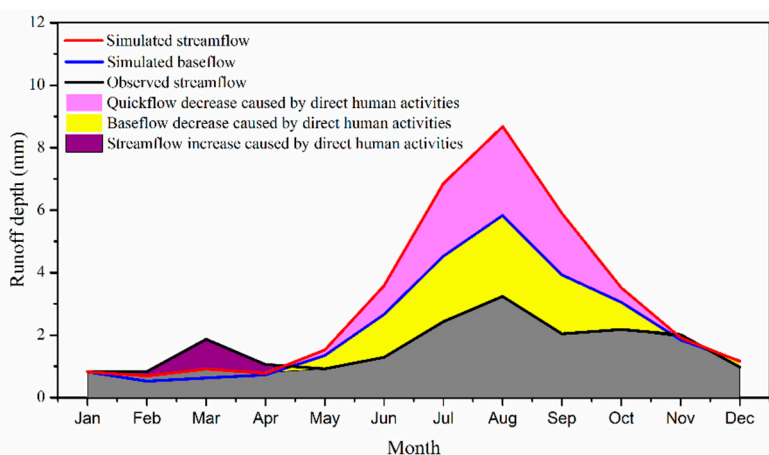


**Figure 12.** Comparison of the simulated streamflow, simulated baseflow and observed streamflow during impact period II (1999–2012).

#### 4.4.3. Contributions of Climate Variability and Human Activities to Streamflow Change

According to the analysis framework described in Section 3.1, the contributions of climate variability and human activities to streamflow decrease were summarized for different impact periods (Table 6). During the total impact period (1980–2012), change in observed average annual streamflow

( $\Delta Q$ ) was  $-46.1$  mm relative to the baseline period (1969–1979). The streamflow change caused by human activities ( $\Delta Q_H$ ) was  $-20.1$  mm, which was calculated by the difference between observed average annual streamflow (33.3 mm) and corresponding simulated value (53.4 mm) during the total impact period. The streamflow change caused by climate variability ( $\Delta Q_C$ ) was  $-26.0$  mm, which was estimated by the difference between  $\Delta Q$  ( $-46.1$  mm) and  $\Delta Q_H$  ( $-20.1$  mm). The contributions of  $\Delta Q_C$  and  $\Delta Q_H$  were 56.4% and 43.6%, respectively.

The streamflow change in the MRB displays different stages. Thus, understanding the contributions of climate variability and human activities to streamflow decrease during different stages is critical for the sustainable utilization of water resource in the MRB. The simulated average annual streamflow were 74.9 mm, 62.9 mm and 40.6 mm for the baseline period, impact period I and II, respectively. Compared to the baseline period, the  $\Delta Q_C$  and  $\Delta Q_H$  were  $-16.5$  mm and  $-19.6$  mm in impact period I, respectively. The contributions of  $\Delta Q_C$  and  $\Delta Q_H$  were 45.7% and 54.3%, respectively. During impact period II,  $\Delta Q_C$  and  $\Delta Q_H$  were  $-38.8$  mm and  $-21.0$  mm, respectively. The climate variability contributed to a decrease of 64.9% in streamflow, while human activities lead to a decrease of 35.1%. Overall, both humans and climate are important driving factors affecting the hydrological processes in the MRB, with human effects having the slight upperhand during 1980–1998 and climate having the upper hand in 1999–2012. In addition, according to equation 4, the streamflow decrease caused by direct human activities resulted in a decrease of 80.5% in human-induced streamflow change in impact period II, which is the ratio of average annual streamflow decrease caused by direct human activities (16.9 mm) to total human-induced streamflow decrease (21 mm).

**Table 6.** Contributions of climate variability and human activities to the streamflow decrease in the MRB during different impact periods.

Period	Q (mm)	$\Delta Q$ (mm)	Qs (mm)	$\Delta Q_C$		$\Delta Q_H$	
				(mm)	%	(mm)	%
Baseline period	79.4	-	74.9	-	-	-	-
Impact period I	43.3	$-36.1$	62.9	$-16.5$	45.7	$-19.6$	54.3
Impact period II	19.6	$-59.8$	40.6	$-38.8$	64.9	$-21.0$	35.1
Total impact period	33.3	$-46.1$	53.4	$-26.0$	56.4	$-20.1$	43.6

Notes: Baseline period, impact period I, impact period II and total impact period refer to the periods of 1969–1979, 1980–1998, 1999–2012 and 1980–2012, respectively. Q is the average annual observed streamflow, Qs is the simulated average annual streamflow and  $\Delta Q$  is the variation of observed average annual streamflow in impact period I, impact period II and total impact period, compared with observed values during baseline period.  $\Delta Q_H$  refers to the difference between observed and simulated average annual runoff during impact period.  $\Delta Q_S$  refers to the difference between  $\Delta Q$  and  $\Delta Q_H$ .

## 5. Discussion

### 5.1. Rationality Analysis of Breakpoint Identification

The existence of these two breakpoints can be rationally explained as follows: (1) Due to the implement of the policy of land reform, and reform and openness in the late 1970s, China experienced rapid social economic development, which caused an increase in regional water consumption [23]. The daily water consumption per capital has been increasing from less than  $0.03$  m<sup>3</sup> in 1959 to more than  $0.1$  m<sup>3</sup> in 1995. Thus, the breakpoint year 1979 is rational. (2) Although the annual precipitation non-significantly reduced during the period of 1969–2012, flood season precipitation decreased at a significant level of 0.05. A breakpoint of flood season precipitation was detected in 1997 (Figure 13), which is based on the heuristic segmentation algorithm. After the year 1999, the MRB experienced constant aridity, which arose from a shortage of precipitation. As indicated in Table 2, the decrease in annual precipitation (flood season precipitation) was 69.7 mm (90.7 mm) relative to baseline period (1969–1979). Meanwhile, water withdrawal significantly increased compared to years before 1999 [25]. The daily water consumption per capital in 2000 was  $0.2$  m<sup>3</sup>, which is twice as much as in 1995.

Thus, the breakpoint year 1998 is rational. Additionally, identification of the breakpoint year 1979 is supported by the work of Wang et al. [23].

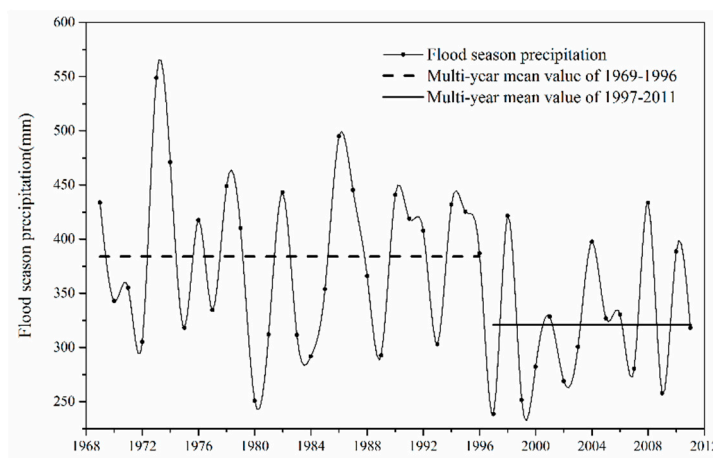


**Figure 13.** Variation of flood season precipitation and its breakpoints in the MRB.

## 5.2. Uncertainty Analysis

The main uncertainties in the climate variability and human activities impacts on streamflow change arise from the breakpoint determination of the streamflow, the length of the study period and simulation uncertainties resulting from the reconstruction of the “natural streamflow” [61]. In this study, the hydrological model, namely SWAT model, was adopted to reconstruct natural streamflow under impact period.

Although the SWAT model performed well in the MRB based on the visual inspection and statistical indicator, there were some discrepancies in the peak events, such as July 1969, which might be attributed to the input data, such as the precipitation data, or the calibration/validation data, uncertainties in the model parameters and/or the model structure [62–64]. Regarding to precipitation data, precipitation data from 11 meteorological stations and 25 rain gauges in and around the study area were used to force the SWAT model, which may still not be enough to represent the spatial variation of precipitation in a study area of 15,400 km<sup>2</sup>. All sources of uncertainty (including input uncertainty, structural uncertainty, parameter uncertainty) were described by parameter uncertainty analysis of streamflow simulation with two statistics: P-factor and R-factor. For the streamflow simulation, the values of P-factor values were greater than 0.71, and R-factor values were lower than 0.6 (except for the validation period at the Zhangjiafen stream-gauging station), indicating a small uncertainty range of simulation results. Because the SWAT-CUP software don't output simulated value of the baseflow and quickflow for each iteration, the uncertainty analysis assessment for baseflow and quickflow simulations could not be performed. However, according to the idea of inputting more available useful information for evaluation to gain less uncertainty [22], it is more likely that a model calibration and validation procedure emphasizing as accurate as possible match between observed and simulated streamflow components will produce a more realistic and robust set of model parameters [65]. For climate change studies, additional uncertainties may come from parameter instability due to the huge difference in climate characteristics between the calibration period and the impact period, further influencing the model robustness [66].

In the framework of identifying the impact of climate variability and human activities on streamflow change, these two driving factors were regarded to be independent. However, these is an interaction between climate variability and human activities in the real world. For example, Daniels et al. [67] used a regional climate model to simulate the effect of land use changes on precipitation in the Netherlands, and found that the simulated effects of land use changes on precipitation in summer are smaller than the effects of climate change, but are not negligible. Therefore,

the interaction between climate variability and human activities need to be further studied to isolate the effects of climate variability and human activities more rationally in the MRB.

### 5.3. Implications for Watershed Management

In the last fifty years, the streamflow into Miyun Reservoir has decreased sharply, which has impacted Beijing's water supply [25,26] and regional ecological environment [24,27]. The studies showed that the streamflow change in the MRB displayed different stages and the contributions of climate variability and human activities to streamflow decrease varied with different stages, which could provide necessary information for water resources management in the watershed. Especially during impact period II (1999–2012), direct human activities, such as water withdrawal, aggravated the decrease in streamflow, future influencing the stream baseflow. Considering the fact that the baseflow has the very important role in river ecosystem stability and health [16], baseflow management should be incorporated in the future water resources management for regional sustainable development. The simulated average monthly baseflow during impact period II (Figure 10) could provide a reference for the establishment of integrated water resources management based on the protection of river baseflow. Similarly, the baseflow decrease caused by human activities at monthly or annual time scales during impact period II (Figure 10) could be considered as a constraint to optimize water resource allocation among various water use sectors or regions and work out a relatively optimum management plan for sustainable utilization of water resource. It should be pointed out that, due to the data limit, the impact of the reservoirs on the streamflow change in the MRB was not separated from the human-induced impacts. In the future work, the reservoir factor will be considered for water resource allocation in the MRB, China. In addition, the reservoir operation will also be considered as the mitigation measure against future climate change in the watershed.

## 6. Conclusions

This study adopted the physically-based hydrological model (SWAT) to determine the individual impact of climate variability and human activities (including direct and indirect human activities) to streamflow change and its contribution and further analyze the impact of human activities on the streamflow by considering the streamflow components in the MRB. In addition, the breakpoint analysis was carried out by heuristic segmentation algorithm, and baseflow separation was conducted by the automatic baseflow filter. The conclusions were drawn as follows:

(1) The annual streamflow responses to climate variability and human activities showed stage changes in the MRB over the past 44 years (1969–2012). That is to say, the period of 1969–2012 was divided into three phases based on the breakpoint analysis: the baseline period (1969–1979), impact period I (1980–1998) and impact period II (1999–2012). Compared to the baseline period, the changes in the magnitude of temperature, precipitation (especially flood season precipitation) and streamflow during impact period II were higher than impact period I.

(2) The climate variability accounted for a decrease of annual streamflow by 16.5 mm and 38.8 mm through the hydrological model (SWAT) during impact period I and II, respectively. The climate variability contributed to 45.7% and 64.9% of the decrease of streamflow into Miyun Reservoir Basin during impact period I and II, respectively.

(3) During impact period II, the direct human activities (mainly including dam construction and reservoir operation, surface and groundwater withdrawal) accounted for a decrease of annual streamflow by 16.9 mm per year on average, which was responsible for 80.5% of human-induced streamflow change. As for streamflow component, baseflow decrease caused by direct human activities was 8.3 mm per year on average.

The decreases in streamflow and baseflow adversely impacted stream ecology and the regional water supply in the Miyun Reservoir Basin. This implies that, under current climate conditions, some immediate measures should be taken to ensure sustainable water resources utilization.

**Supplementary Materials:** The following are available online at <http://www.mdpi.com/2071-1050/10/4/941/s1>, Figure S1: The land use of the MRB in 1980s and 2000, Table S1: The information of the reservoirs in the watershed, Table S2: Hydrology stations, rainfall gauges and meteorological stations used in the watershed, Table S3: Calibrated parameters and their initial range and calibrated value in the watershed.

**Acknowledgments:** This research was funded by the National Science Foundation for Innovative Research Group (No. 51721093), the National Science Foundation of China (No. 51579011) and Newton Fund (Grant Ref: BB/N013484/1).

**Author Contributions:** All authors contributed to the design and development of this manuscript. Tiezhu Yan performed the data analysis and prepared the first draft of the manuscript. Amelia LEE ZHI YI gathered the data information. Zhenyao Shen provided the original ideas and improved the discussion, and Jianwen Bai edited the manuscript prior to submission.

**Conflicts of Interest:** The authors declare no conflict of interest.

## References

- Huntington, T.G. Evidence for intensification of the global water cycle: Review and synthesis. *J. Hydrol.* **2006**, *319*, 83–95. [[CrossRef](#)]
- Milly, P.C.D.; Dunne, K.A.; Vecchia, A.V. Global pattern of trends in streamflow and water availability in a changing climate. *Nature* **2005**, *438*, 347–350. [[CrossRef](#)] [[PubMed](#)]
- Lahmer, W.; Pftzner, B.; Becker, A. Assessment of land use and climate change impacts on the mesoscale. *Phys. Chem. Earth Part B Hydrol. Oceans Atmos.* **2001**, *26*, 565–575. [[CrossRef](#)]
- Milliman, J.D.; Farnsworth, K.L.; Jones, P.D.; Xu, K.H.; Smith, L.C. Climatic and anthropogenic factors affecting river discharge to the global ocean, 1951–2000. *Glob. Planet. Chang.* **2008**, *62*, 187–194. [[CrossRef](#)]
- Poff, N.L.; Allan, J.D.; Bain, M.B.; Karr, J.R.; Prestegard, K.L.; Richter, B.D.; Sparks, R.E.; Stromberg, J.C. The natural flow regime. *Bioscience* **1997**, *47*, 769–784. [[CrossRef](#)]
- Feng, X.; Zhang, G.; Yin, X. Hydrological Responses to Climate Change in Nenjiang River Basin, Northeastern China. *Water Res. Manag.* **2011**, *25*, 677–689. [[CrossRef](#)]
- Hao, X.; Chen, Y.; Xu, C.; Li, W. Impacts of climate change and human activities on the surface runoff in the Tarim River basin over the last fifty years. *Water Res. Manag.* **2008**, *22*, 1159–1171. [[CrossRef](#)]
- Dey, P.; Mishra, A. Separating the impacts of climate change and human activities on streamflow: A review of methodologies and critical assumptions. *J. Hydrol.* **2017**, *548*, 278–290. [[CrossRef](#)]
- Zhang, K.; Li, L.; Bai, P.; Li, J.; Liu, Y. Influence of climate variability and human activities on stream flow variation in the past 50 years in Taoer River, Northeast China. *J. Geogr. Sci.* **2017**, *27*, 481–496. [[CrossRef](#)]
- Kliment, Z.; Matouskova, M. Runoff Changes in the umava Mountains (Black Forest) and the Foothill Regions: Extent of Influence by Human Impact and Climate Change. *Water Res. Manag.* **2009**, *23*, 1813–1834. [[CrossRef](#)]
- Patterson, L.A.; Lutz, B.; Doyle, M.W. Climate and direct human contributions to changes in mean annual streamflow in the South Atlantic, USA. *Water Res. Res.* **2013**, *49*, 7278–7291. [[CrossRef](#)]
- Wang, D.; Hejazi, M. Quantifying the relative contribution of the climate and direct human impacts on mean annual streamflow in the contiguous United States. *Water Resour. Res.* **2011**, *47*, 1–16. [[CrossRef](#)]
- Lin, K.; Guo, S.; Zhang, W.; Liu, P. A new baseflow separation method based on analytical solutions of the Horton infiltration capacity curve. *Hydrol. Process.* **2007**, *21*, 1719–1736. [[CrossRef](#)]
- Zheng, M. Estimation of base flow using flow-sediment relationships in the Chinese Loess Plateau. *Catena* **2015**, *125*, 129–134. [[CrossRef](#)]
- Merz, R.; Bloeschl, G.; Parajka, J. Spatio-temporal variability of event runoff coefficients. *J. Hydrol.* **2006**, *331*, 591–604. [[CrossRef](#)]
- Price, K. Effects of watershed topography, soils, land use, and climate on baseflow hydrology in humid regions: A review. *Prog. Phys. Geogr.* **2011**, *35*, 465–492. [[CrossRef](#)]
- Zhang, X.S.; Srinivasan, R.; Arnold, J.; Izaurrealde, R.C.; Bosch, D. Simultaneous calibration of surface flow and baseflow simulations: A revisit of the SWAT model calibration framework. *Hydrol. Process.* **2011**, *25*, 2313–2320. [[CrossRef](#)]
- Zhang, A.; Zhang, C.; Fu, G.; Wang, B.; Bao, Z.; Zheng, H. Assessments of Impacts of Climate Change and Human Activities on Runoff with SWAT for the Huifa River Basin, Northeast China. *Water Res. Manag.* **2012**, *26*, 2199–2217. [[CrossRef](#)]

19. Lee, G.; Shin, Y.; Jung, Y. Development of Web-Based RECESS Model for Estimating Baseflow Using SWAT. *Sustainability* **2014**, *6*, 2357–2378. [[CrossRef](#)]
20. Luo, Y.; Arnold, J.; Allen, P.; Chen, X. Baseflow simulation using SWAT model in an inland river basin in Tianshan Mountains, Northwest China. *Hydrol. Earth Syst. Sci.* **2012**, *16*, 1259–1267. [[CrossRef](#)]
21. Shi, P.; Chen, C.; Srinivasan, R.; Zhang, X.S.; Cai, T.; Fang, X.Q.; Qu, S.M.; Chen, X.; Li, Q.F. Evaluating the SWAT Model for Hydrological Modeling in the Xixian Watershed and a Comparison with the XAJ Model. *Water Res. Manag.* **2011**, *25*, 2595–2612. [[CrossRef](#)]
22. Lin, K.; Lian, Y.; He, Y. Effect of Baseflow Separation on Uncertainty of Hydrological Modeling in the Xinanjiang Model. *Math. Probl. Eng.* **2014**, *2014*, 1–9. [[CrossRef](#)]
23. Wang, G.; Xia, J.; Chen, J. Quantification of effects of climate variations and human activities on runoff by a monthly water balance model: A case study of the Chaobai River basin in northern China. *Water Resour. Res.* **2009**, *45*, 1–12. [[CrossRef](#)]
24. Wang, X.; Hao, G.; Yang, Z.; Liang, P.; Cai, Y.; Li, C.; Sun, L.; Zhu, J. Variation analysis of streamflow and ecological flow for the twin rivers of the Miyun Reservoir Basin in northern China from 1963 to 2011. *Sci. Total Environ.* **2015**, *536*, 739–749. [[CrossRef](#)] [[PubMed](#)]
25. Ma, H.; Yang, D.; Tan, S.K.; Gao, B.; Hu, Q. Impact of climate variability and human activity on streamflow decrease in the Miyun Reservoir catchment. *J. Hydrol.* **2010**, *389*, 317–324. [[CrossRef](#)]
26. Yan, T.; Shen, Z.; Bai, J. Spatial and Temporal Changes in Temperature, Precipitation, and Streamflow in the Miyun Reservoir Basin of China. *Water* **2017**, *9*. [[CrossRef](#)]
27. Tang, L.; Yang, D.; Hu, H.; Gao, B. Detecting the effect of land-use change on streamflow, sediment and nutrient losses by distributed hydrological simulation. *J. Hydrol.* **2011**, *409*, 172–182. [[CrossRef](#)]
28. Zhao, Y.; Zhang, X.; Cao, W.; Yu, X.; Liu, B.; Zhu, B.; Cheng, C.; Yin, X.; Xie, G. Effect of climatic change and afforestation on water yield in the Rocky Mountain Area of North China. *For. Syst.* **2015**, *24*. [[CrossRef](#)]
29. Zheng, J.; Sun, G.; Li, W.; Yu, X.; Zhang, C.; Gong, Y.; Tu, L. Impacts of land use change and climate variations on annual inflow into the Miyun Reservoir, Beijing, China. *Hydrol. Earth Syst. Sci.* **2016**, *20*, 1561–1572. [[CrossRef](#)]
30. Reddy, A.S.; Reddy, M.J. Evaluating the influence of spatial resolutions of DEM on watershed runoff and sediment yield using SWAT. *J. Earth Syst. Sci.* **2015**, *124*, 1517–1529. [[CrossRef](#)]
31. Tan, M.L.; Ficklin, D.L.; Dixon, B.; Ibrahim, A.L.; Yusop, Z.; Chaplot, V. Impacts of DEM resolution, source, and resampling technique on SWAT-simulated streamflow. *Appl. Geogr.* **2015**, *63*, 357–368. [[CrossRef](#)]
32. Wang, H.Q.; Zhang, M.S.; Zhu, H.; Dang, X.Y.; Yang, Z.; Yin, L.H. Hydro-climatic trends in the last 50 years in the lower reach of the Shiyang River Basin, NW China. *Catena* **2012**, *95*, 33–41. [[CrossRef](#)]
33. Wang, W.; Shao, Q.; Yang, T.; Peng, S.; Xing, W.; Sun, F.; Luo, Y. Quantitative assessment of the impact of climate variability and human activities on runoff changes: A case study in four catchments of the Haihe River basin, China. *Hydrol. Process.* **2013**, *27*, 1158–1174. [[CrossRef](#)]
34. Ye, X.; Zhang, Q.; Liu, J.; Li, X.; Xu, C.-Y. Distinguishing the relative impacts of climate change and human activities on variation of streamflow in the Poyang Lake catchment, China. *J. Hydrol.* **2013**, *494*, 83–95. [[CrossRef](#)]
35. Li, Y.; Chang, J.; Wang, Y.; Jin, W.; Guo, A. Spatiotemporal Impacts of Climate, Land Cover Change and Direct Human Activities on Runoff Variations in the Wei River Basin, China. *Water* **2016**, *8*. [[CrossRef](#)]
36. Huang, S.; Huang, Q.; Leng, G.; Zhao, M.; Meng, E. Variations in annual water-energy balance and their correlations with vegetation and soil moisture dynamics: A case study in the Wei river basin, China. *J. Hydrol.* **2017**, *546*, 515–525. [[CrossRef](#)]
37. Zhang, J.; Huang, Q.; Zhao, X. Comparative research on abrupt change analysis methods for hydrological time series in Zhangze reservoir. *J. Basic Sci. Eng.* **2013**, *21*, 837–844. (In Chinese)
38. Liu, Q.; Wan, S.; Gu, B. A review of the detection methods for climate regime shifts. *Discret. Dyn. Nat. Soc.* **2016**. [[CrossRef](#)]
39. Bernaola-Galvan, P.; Ivanov, P.C.; Amaral, L.A.N.; Stanley, H.E. Scale invariance in the nonstationarity of human heart rate. *Phys. Rev. Lett.* **2001**. [[CrossRef](#)] [[PubMed](#)]
40. Huang, S.; Chang, J.; Huang, Q.; Wang, Y.; Chen, Y. Calculation of the instream ecological flow of the Wei river based on hydrological variation. *J. Appl. Math.* **2014**. [[CrossRef](#)]
41. Qian, B.; Zhang, D.; Wang, J.; Huang, F.; Wu, Y. Impacts of reservoirs on the streamflow and sediment load of the Hanjiang river, China. *Environ. Monit. Assess.* **2016**, *188*, 1–10. [[CrossRef](#)] [[PubMed](#)]

42. Huang, F.; Xia, Z.; Li, F.; Wu, T. Assessing sediment regime alteration of the upper Yangtze river. *Environ. Earth Sci.* **2013**, *70*, 2349–2357. [[CrossRef](#)]
43. Neitsch, S.L.; Arnold, J.G.; Kiniry, J.R.; Williams Grassland, J.R. *Soil and Water Assessment Tool Theoretical Documentation Version 2009*; Texas Water Resources Institute: Temple, TX, USA, 2011.
44. Arnold, J.G.; Fohrer, N. Swat2000: Current capabilities and research opportunities in applied watershed modelling. *Hydrol. Process.* **2005**, *19*, 563–572. [[CrossRef](#)]
45. Gassman, P.W.; Sadeghi, A.M.; Srinivasan, R. Applications of the swat model special section: Overview and insights. *J. Environ. Qual.* **2014**, *43*, 1–8. [[CrossRef](#)] [[PubMed](#)]
46. Shen, Z.; Zhong, Y.; Huang, Q.; Chen, L. Identifying non-point source priority management areas in watersheds with multiple functional zones. *Water Res.* **2015**, *68*, 563–571. [[CrossRef](#)] [[PubMed](#)]
47. Zhang, L.; Li, X. Assessing hydrological effects of human activities by hydrological characteristic parameters: A case study in the Yunzhou reservoir basin. *Res. Sci.* **2004**, *26*, 62–67. (In Chinese)
48. Zhu, L.; Qin, F.; Yao, Y. Response of land use change to hydrological dynamics in rocky mountain area of north china based on Yunzhou reservoir of Zhangjiakou. *Res. Soil Water Conserv.* **2009**, *16*, 224–228. (In Chinese)
49. Abbaspour, K.C.; Vejdani, M.; Haghighat, S. Swat-cup calibration and uncertainty programs for swat. *Modsim 2007 Int. Congr. Model. Simul. Land Water Environ. Manag. Integr. Syst. Sustain.* **2007**, 1603–1609. [[CrossRef](#)]
50. Yang, J.; Reichert, P.; Abbaspour, K.C.; Xia, J.; Yang, H. Comparing uncertainty analysis techniques for a swat application to the chaohe basin in china. *J. Hydrol.* **2008**, *358*, 1–23. [[CrossRef](#)]
51. Moriasi, D.N.; Arnold, J.G.; Van Liew, M.W.; Bingner, R.L.; Harmel, R.D.; Veith, T.L. Model evaluation guidelines for systematic quantification of accuracy in watershed simulations. *Trans. ASABE* **2007**, *50*, 885–900. [[CrossRef](#)]
52. Partington, D.; Brunner, P.; Simmons, C.T.; Werner, A.D.; Therrien, R.; Maier, H.R.; Dandy, G.C. Evaluation of outputs from automated baseflow separation methods against simulated baseflow from a physically based, surface water-groundwater flow model. *J. Hydrol.* **2012**, *458*, 28–39. [[CrossRef](#)]
53. He, S.; Li, S.; Xie, R.; Lu, J. Baseflow separation based on a meteorology-corrected nonlinear reservoir algorithm in a typical rainy agricultural watershed. *J. Hydrol.* **2016**, *535*, 418–428. [[CrossRef](#)]
54. Arnold, J.G.; Allen, P.M.; Muttiah, R.; Bernhardt, G. Automated base-flow separation and recession analysis techniques. *Ground Water* **1995**, *33*, 1010–1018. [[CrossRef](#)]
55. Vincent, L.; Hollick, M. *Stochastic Time-Variable Rainfall-Runoff Modelling*; Hydrology and Water Resources Symposium Perth 1979 Proceedings; National Committee on Hydrology and Water Resources of the Institution of Engineers: Hobart, Australia, 1979; pp. 89–92.
56. Arnold, J.G.; Allen, P.M. Automated methods for estimating baseflow and ground water recharge from streamflow records. *J. Am. Water Resour. Assoc.* **1999**, *35*, 411–424. [[CrossRef](#)]
57. Li, L.; Maier, H.R.; Lambert, M.P.; Simmons, C.T.; Partington, D. Framework for assessing and improving the performance of recursive digital filters for baseflow estimation with application to the lyne and hollick filter. *Environ. Model. Softw.* **2013**, *41*, 163–175. [[CrossRef](#)]
58. Huang, X.-D.; Shi, Z.-H.; Fang, N.-F.; Li, X. Influences of land use change on baseflow in mountainous watersheds. *Forests* **2016**, *7*. [[CrossRef](#)]
59. Gan, R.; Sun, L.; Luo, Y. Baseflow characteristics in alpine rivers—A multi-catchment analysis in northwest china. *J. Mt. Sci.* **2015**, *12*, 614–625. [[CrossRef](#)]
60. Ahiablame, L.; Chaubey, I.; Engel, B.; Cherkauer, K.; Merwade, V. Estimation of annual baseflow at ungauged sites in indiana USA. *J. Hydrol.* **2013**, *476*, 13–27. [[CrossRef](#)]
61. Bao, Z.; Zhang, J.; Wang, G.; Fu, G.; He, R.; Yan, X.; Jin, J.; Liu, Y.; Zhang, A. Attribution for decreasing streamflow of the haihe river basin, northern china: Climate variability or human activities? *J. Hydrol.* **2012**, *460*, 117–129. [[CrossRef](#)]
62. Shen, Z.Y.; Chen, L.; Chen, T. Analysis of parameter uncertainty in hydrological and sediment modeling using glue method: A case study of swat model applied to three gorges reservoir region, china. *Hydrol. Earth Syst. Sci.* **2012**, *16*, 121–132. [[CrossRef](#)]
63. Shrestha, B.; Cochrane, T.A.; Caruso, B.S.; Arias, M.E.; Piman, T. Uncertainty in flow and sediment projections due to future climate scenarios for the 3s rivers in the mekong basin. *J. Hydrol.* **2016**, *540*, 1088–1104. [[CrossRef](#)]

64. Yen, H.; Wang, X.; Fontane, D.G.; Harmel, R.D.; Arabi, M. A framework for propagation of uncertainty contributed by parameterization, input data, model structure, and calibration/validation data in watershed modeling. *Environ. Model. Softw.* **2014**, *54*, 211–221. [[CrossRef](#)]
65. Rouhani, H.; Willems, P.; Wyseure, G.; Feyen, J. Parameter estimation in semi-distributed hydrological catchment modelling using a multi-criteria objective function. *Hydrol. Process.* **2007**, *21*, 2998–3008. [[CrossRef](#)]
66. Brigode, P.; Oudin, L.; Perrin, C. Hydrological model parameter instability: A source of additional uncertainty in estimating the hydrological impacts of climate change? *J. Hydrol.* **2013**, *476*, 410–425. [[CrossRef](#)]
67. Daniels, E.; Lenderink, G.; Hutjes, R.; Holtslag, A. Relative impacts of land use and climate change on summer precipitation in the netherlands. *Hydrol. Earth Syst. Sci.* **2016**, *20*, 4129–4142. [[CrossRef](#)]



© 2018 by the authors. Licensee MDPI, Basel, Switzerland. This article is an open access article distributed under the terms and conditions of the Creative Commons Attribution (CC BY) license (<http://creativecommons.org/licenses/by/4.0/>).